Biology of Reproduction, 2019, 101(4), 771–781
doi:10.1093/biolre/ioz116
Research Article
Advance Access Publication Date: 10 July 2019

Research Article

Developmental origins of ovarian disorder: impact of maternal lean gestational diabetes on the offspring ovarian proteome in mice†

Kendra L. Clark[1], Omonseigho O. Talton[2], Shanthi Ganesan[1], Laura C. Schulz[2] and Aileen F. Keating[1,*]

[1]Department of Animal Science, Iowa State University, Ames, Iowa, USA and [2]Department of Obstetrics, Gynecology, and Women's Health, University of Missouri, Columbia, Missouri, USA

***Correspondence:** Department of Animal Science, Iowa State University, 2356H Kildee Hall, Ames, Iowa 50011, USA. Tel: 515-509-3849 Fax: 515-509-4471, E-mail: akeating@iastate.edu

† **Grant Support:** This work was in part funded by the Bailey Career Development Award from Iowa State University (AFK).
Conference Presentation: Presented in part at the 51st Annual Society for the Study of Reproduction (SSR) meeting, July 10–13, 2018, New Orleans, Louisiana.

Received 19 March 2019; Revised 6 January 2019; Accepted 4 July 2019

Abstract

Gestational diabetes mellitus (GDM) is an obstetric disorder affecting approximately 10% of pregnancies. The four high-fat, high-sucrose (HFHS) mouse model emulates GDM in lean women. Dams are fed a HFHS diet 1 week prior to mating and throughout gestation resulting in inadequate insulin response to glucose in mid-late pregnancy. The offspring of HFHS dams have increased adiposity, thus, we hypothesized that maternal metabolic alterations during lean GDM would compromise ovarian function in offspring both basally and in response to a control or HFHS diet in adulthood. Briefly, D_LP_L were lean dams and control diet pups; D_LP_H were lean dams and HFHS pups; D_HP_L were HFHS dams and control diet pups; and D_HP_H were HFHS dams and HFHS pups. A HFHS challenge in the absence of maternal GDM (D_LP_L vs. D_LP_H) increased 3 and decreased 30 ovarian proteins. Maternal GDM in the absence of a dietary stress (D_LP_L vs. D_HP_L) increased abundance of 4 proteins and decreased abundance of 85 proteins in the offspring ovary. Finally, 87 proteins increased, and 4 proteins decreased in offspring ovaries due to dietary challenge and exposure to maternal GDM in utero (D_LP_L vs. D_HP_H). Canopy FGF signaling regulator 2, deleted in azoospermia-associated protein 1, septin 7, and serine/arginine-rich splicing factor 2 were altered across multiple offspring groups. Together, these findings suggest a possible impact on fertility and oocyte quality in relation to GDM exposure in utero as well as in response to a western diet in later life.

Summary Sentence

Altered abundance of ovarian proteins in offspring who experienced maternal GDM highlights the potential long-term effects of metabolic changes on ovarian function.

Key words: gestational diabetes, ovary, proteomics, offspring health

Introduction

The ovary produces the female gamete, the oocyte, and primary sex hormones 17β-estradiol (E_2), and progesterone (P_4). Oocytes arise from primordial germ cells in utero and remain encased in primitive follicular structures and arrested at the diplotene stage of meiosis, or they degenerate through programmed cell death termed atresia [1]. Through the natural progression of time or due to factors that may expedite the process, the pool of ovarian oocytes ultimately becomes depleted and ovarian senescence occurs in women [1]. Ovarian failure preceding age 40 is characterized as primary ovarian insufficiency (POI) [2], which may be attributable to genetics, autoimmune disorders, iatrogenesis, surgical, or unknown etiology, and affects approximately 1% of women [3].

In recent years, globally there has been an expeditious rise in obesity rates in both adults and children, predisposing them for health problems including diabetes [4], cardiovascular disease [5], cancer [6], and reproductive decline [7]. In the overweight or obese female, reproductive complications include POI [8], polycystic ovary syndrome (PCOS) [9], poor oocyte quality [10], decreased fecundity [11], gestational diabetes mellitus (GDM) [12], and offspring congenital abnormalities [13]. Changes in central metabolism negatively affect the ovary, with insulin responsive pathways such as the phosphatidylinositol 3-kinase (PI3K) pathway being upregulated during obesity [14], reduced follicle number [15], altered steroid hormone biosynthesis [16], and inflammation [15]. Additionally, basal ovarian DNA damage and a blunted ovarian response to genotoxicants occurs in obese mice [16–19]. Offspring exposed to maternal obesity have increased risk of neural tube defects [20], glucose intolerance [21], altered neurobehavior [22], intrauterine growth restriction (IUGR) [23], and increased circulating cholesterol and body fat [24]. The reproductive outcomes on female offspring exposed to maternal obesity in utero include a decrease in the ovarian follicular reserve [25, 26], decreases in ovarian vascularity [27], and disturbances in the estrous cycle in a rodent model [28].

In association to the rise of obesity in reproductive age women, the prevalence of GDM is also increasing. Defined as glucose intolerance during pregnancy, GDM may affect up to 20% of pregnancies, dependent on population demographics [29], screening and diagnostic criteria [29], and pregestational maternal lifestyle factors [30]. Insulin sensitivity naturally decreases during pregnancy for all women [31], but overweight and obese women have higher risk of developing GDM than their lean counterparts [12, 32], and lean women with GDM have reduced or delayed first-phase insulin response to glucose [31]. Immediate health concerns are posed by GDM, and although GDM normally resolves postpartum, long-term maternal health effects include a 60% higher risk of acquiring type 2 diabetes [33, 34]. Fetal and neonatal complications include macrosomia [35], hypoglycemia [36], respiratory distress [36], future obesity [37], and predisposition for type 2 diabetes [38].

When considering our recent findings that progressive obesity alters a variety of ovarian intracellular signaling pathways that could compromise fertility and offspring health [14, 15, 17, 19, 39, 40], we hypothesized that similar alterations would result from exposure of the developing ovary to metabolic alterations in utero. A lean GDM model has been developed using acute, high-fat feeding 1 week prior to conception and throughout gestation, thereby separating effects of preconceptional obesity from maternal gestational metabolic alterations on the offspring [41]. We utilized ovaries from offspring who experienced GDM in utero and also assessed whether a dietary stress in adulthood would affect the ovarian response to such an insult.

Materials and methods

Animal procedures and tissue collection

Ovarian tissue utilized in this study was obtained as part of a larger study [42]. Briefly, gestational diabetes was induced in female C57B16/J mice ($n = 14$) by feeding a high-fat, high-sucrose (HFHS; 45% kcal/fat (lard and soybean oil) and 17% kcal/sucrose) diet (D12451, Research Diets, Inc.) 1 week prior to mating and for the duration of gestation, for a total of 4 weeks as described [41, 42]. Control female C57B16/J mice (Jackson Laboratories; $n = 20$) were fed a chow breeder diet (17% kcal/fat (lard) and 2.4% kcal/sucrose; LabDiet 5008, Purina) throughout the duration of the study. Both groups of females were mated to C57B16/J sires. Female offspring from each litter (control—$n = 30$; GDM—$n = 16$) were maintained on the chow breeder diet, until 23 weeks of age, at which point 1–2 females from each litter was fed the HFHS diet until 31 weeks of age, at which time both groups of offspring were humanely sacrificed. Mice were not at the same stage of the estrous cycle at euthanasia. Ovaries were collected from adult females and one ovary was snap frozen in liquid nitrogen before storage at −80 °C. The contralateral ovary was fixed in 4% paraformaldehyde and stored in 70% ethanol prior to histological processing. Ovaries utilized for frozen tissue sections were collected from 10-week-old female C57B16/J mice during the proestrus stage of the estrous cycle and fixed in 4% paraformaldehyde overnight at 4 °C. For cryoprotection, fixed ovaries were passed in 10% sucrose/PBS solution for 1–3 h at room temperature followed by 30% sucrose/PBS solution at 4 °C overnight prior to embedding in OCT medium (Fisher Healthcare). All animal procedures were approved by the University of Missouri or the Iowa State University Institutional Animal Care and Use Committee and handled according to National Institutes of Health Guide for Care and Use of Laboratory Animals.

Histology and follicle counting

Fixed ovaries were paraffin embedded and serially sectioned ($n = 4$/treatment) at 5 µm, with every sixth section mounted onto glass slides and stained with hematoxylin and eosin. Healthy follicles containing oocytes with a distinct oocyte nucleus were counted and classified as follows: primordial follicles were identified by an oocyte surrounded by a single layer of squamous granulosa cells; primary follicles contained the oocyte surrounded by a single layer of cuboidal granulosa cells; and secondary follicles contained an oocyte surrounded by multiple layers of granulosa cells. Slide identity was blinded to prevent counting bias. Follicle counts performed on a Nikon Optiphot using a 5× or 20× objective, and bright field images captured on an inverted DMI3000B microscope (Leica) and QICAM MicroPublisher 5.0 (MP5.0-RTV-CLR-10, QIMAGING) camera using QCapture software at a 5× objective. Total follicles counted per ovary were compared between treatments.

Protein isolation, LC–MS/MS, and proteome analysis

Total ovarian protein was isolated ($n = 3$/treatment) in lysis buffer (50 mM Tris-HCL, 1 mM EDTA, pH 8.5), homogenized, and centrifuged at 10 000 rpm at 4 °C for 15 min. Supernatant was collected, and protein content was quantified using bicinchoninic acid assay (BCA; Pierce BCA Protein Assay Kit, Thermofisher). A working protein dilution of 50 µg/µL was prepared with lysis buffer. For liquid chromatography–tandem mass spectrometry (LC–MS/MS) analysis, total protein (50 µg/µL) was digested with trypsin/Lys-C for 16 h, dried down, and reconstituted in buffer A (47.5 µL, 0.1%

formic acid/water), and Peptide Retention Time Calibration (PRTC) mixture was utilized as a standard (25 fmol/μL) and was spiked into each sample to serve as an internal control. Protein (10 μg) and PRTC (250 fmol) were injected onto a liquid chromatography column (Agilent Zorbax SB-C18, 0.5 mm × 150 mm, 5 micron) using an Agilent 1260 Infinity Capillary Pump. Peptides were separated by liquid chromatography and analyzed using a Q Exactive Hybrid Quadrupole-Orbitrap Mass Spectrometer with a higher energy collisional dissociation fragmentation cell. The resulting intact and fragmentation pattern was compared to a theoretical fragmentation pattern (from either MASCOT or Sequest HT) to identify peptides. The relative abundance of the identified proteins was based on the areas of the top three unique peptides for each sample. The arithmetic mean of the PRTC was used as normalization factor. For each peptide, the signal intensity was divided by the arithmetic mean of the PRTC before further analysis.

Metaboanalyst 3.0 [43, 44] was used for data analysis. Upon finding data integrity to be satisfactory (no peptide with more than 50% missing replicates, positive values for the area), missing value imputation was performed using a singular value decomposition method. Filtering, based on interquartile range, was performed to remove values unlikely to be of use when modeling the data, followed by generalized log transformation (glog 2) before data analysis. The control and treatment samples were compared by the Student *t*-test. Differences between groups were assessed by the Mann-Whitney rank sum test. All *P*-values were two sided. To adjust for multiple comparisons, Bonferroni correction was applied and only *P*-values less than 0.1 were considered as statistically significant. The principal component analysis was performed using the *prcomp* package and pairwise score plots providing an overview of the various separation patterns among the most significant components were accessed. The partial least squares (PLS) regression was then performed using the *plsr* function provided by R *pls* package. The classification and cross validation were also performed using the *caret* package. The UniProt protein identifiers that were up/down regulated were used to retrieve the corresponding KEGG identifiers using the "Retrieve/ID mapping" tool of UniProt (accessible at https://www.uniprot.org/uploadlists/). KEGG identifiers were then used to retrieve biological pathway association of the proteins.

Gene ontology analysis

Gene ontology (GO) analysis was performed using PANTHER version 14.1 (http://www.pantherdb.org). Proteins identified in the control and experimental samples were compared to the *Mus musculus* reference list for a statistical overrepresentation test to highlight categories in biological process, molecular function, and cellular components with significant fold enrichment in our samples. The Fisher exact test with false discovery rate (FDR) correction was used with $P < 0.05$ considered as a statistically significant difference.

Immunofluorescence staining

Slides were deparaffinized in Citrisolv and rehydrated in subsequent washes of ethanol (100, 95, and 75%), followed by one wash in ddH_2O. Heat-mediated antigen retrieval was performed using citrate buffer (10 mM citric acid, 0.5% Tween20, pH 6.0) in a microwave for 22 min. Tissue sections on histology slides were encircled with a histology pap pen to keep liquid concentrated on the tissue during processing, followed by the application of blocking solution (0.1 M PBS/0.4% BSA/0.2% Tween20/2.5% goat serum) to the slides for 1 h at room temperature. In addition, frozen tissue from 10-week-old female C57B16/J mice was utilized to determine localization of canopy FGF signaling regulator 2 (CNPY2), deleted in azoospermia-associated protein 1 (DAZAP1), pre-mRNA serine/arginine rich splicing factor 2 (SRSF2), and septin 7 (SEPT7). Briefly, frozen slides were thawed on a 37 °C slide warmer for 5 min, tissue encircled with a histology pap pen, and rehydrated in phosphate buffered saline with 0.1% Tween20 (PBSTw) for 20 min at room temperature before addition of blocking solution (described above). Primary antibodies for CNPY2, DAZAP1, SRSF2, SEPT7, phosphorylated histone 2AX (γH2AX), and cleaved caspase-3 (CASP3; dilutions listed in Supplementary Table 1) were added into fresh blocking solution, applied to tissue sections, and allowed to incubate in a humidified box at 4 °C overnight. Slides were washed (3 × 10 min) in PBSTw. Secondary antibodies (Supplementary Table 1) were added into fresh blocking solution and incubated at room temperature for 60 min, followed by washes (3 × 10 min) in PBSTw. Slides were allowed to air dry, counterstained and mounted with 4–6-diamidino-2-phenyllindole (DAPI), and stored at 4 °C until image capture. Negative technical controls to confirm specificity were performed using secondary antibodies alone (Supplementary Figure 4). Images were captured on a Zeiss LSM700 confocal microscope equipped with an AxioCam MRc5 using a 20× objective lens. For γH2AX ($n = 4$ ovaries per treatment; three sections per ovary; sections selected randomly) and cleaved CASP3 ($n = 4$ ovaries per treatment; three sections per ovary; sections selected randomly), immunopositive cells were manually counted in the granulosa cells and/or oocytes of primary, secondary, and antral follicles using the cell counter module of ImageJ (https://imagej.nih.gov/ij/plugins/cell-counter.html).

Statistical analysis

Statistical analyses were performed using GraphPad Prism 7.0 one-way analysis of variance (One-way ANOVA) function with multiple comparisons. Each treatment mean value was compared to the control (D_LP_L) mean value using Dunnett's correction with significance level set at $P \leq 0.05$.

Results

GDM exposure in utero and subsequent dietary challenge decreased healthy follicle number

The impact of GDM exposure in utero and/or dietary stressor later in life on healthy follicle numbers was determined (Figure 1). There was no difference in primordial follicle number between treatment groups (D_LP_H; D_HP_L; and D_HP_H) relative to D_LP_L control ($P = 0.1361$; Figure 1A). Dietary stress in adulthood in the D_LP_H mice did not impact primordial, primary, or secondary follicle number (Figure 1A–C). GDM exposure in utero also did not affect primordial, primary, or secondary follicle number (Figure 1A–C). The combination of GDM in utero with dietary stress in adulthood in the D_HP_H mice numerically reduced primordial follicle number (Figure 1A) and decreased ($P < 0.05$) the number of primary and secondary follicles (Figure 1B and C).

Impact of in utero exposure to GDM on DNA damage in the ovary

To determine if offspring from GDM mothers had increased ovarian DNA damage, tissue sections were immunologically stained for γH2AX and positive foci were quantified. The number of ovarian cells (granulosa cells and/or oocytes) that contained positive γH2AX foci in the primary, secondary, or antral follicles were not different

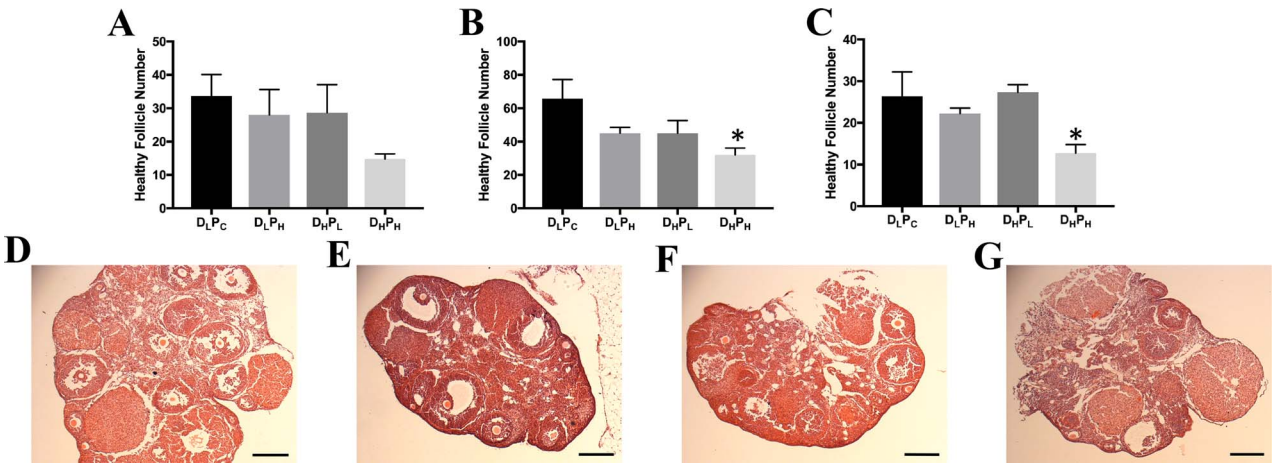

Figure 1. Effect of GDM and/or HFHS diet on ovarian follicle number. Follicles were classified as (A) primordial; (B) primary; and (C) secondary and counted. Bars represent mean counted follicle number ± SEM. Significant difference from D_LP_L control is indicated by the * symbol at = $P < 0.05$. Representative hematoxylin and eosin stained ovarian sections from (D) D_LP_L; (E) D_LP_H; (F) D_HP_L; and (G) D_HP_H are presented; scale bar = 200 µm.

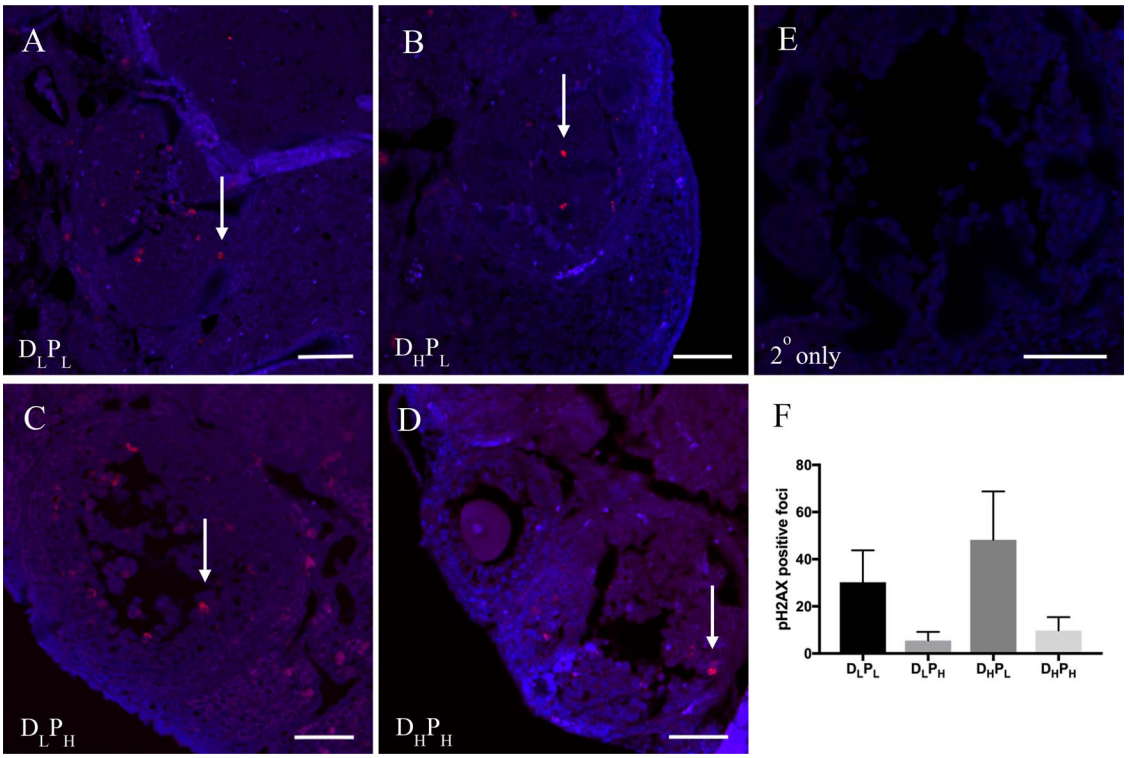

Figure 2. Effect of GDM and/or dietary stress on ovarian γH2AX. A primary antibody directed against γH2AX was used to determine ovarian localization in (A) D_LP_L; (B) D_HP_L; (C) D_LP_H; and (D) D_HP_H mice. (E) Secondary antibody only control. Red punctate staining indicates γH2AX while cellular DNA is stained in blue; scale bar = 50 µm. Arrows indicate γH2AX-positive staining in the granulosa cells of secondary follicles. (F) The bars represent mean number of positive γH2AX foci ± SEM; *n* = 4 ovaries per treatment; three sections per ovary.

between treatment groups (D_LP_L: 30.1 ± 13.5; D_LP_H: 5.5 ± 3.6; D_HP_L: 48.3 ± 20.5; D_HP_H: 9.8 ± 5.7; Figure 2A–F).

Impact of in utero exposure to GDM on apoptosis in the ovary

In order to assess levels of apoptosis in the ovary, immunofluorescence staining was performed to quantify the level of cleaved CASP3. There was no impact of GDM exposure in utero or dietary stress on any treatment group in the level of cleaved CASP3 that was detected in the granulosa cells or oocytes of primary, secondary, or antral follicles (D_LP_L: 8.8 ± 2.1; D_LP_H: 12 ± 2.2; D_HP_L: 10.3 ± 3; D_HP_H: 13 ± 7.6; Figure 3A–F).

In utero exposure to lean GDM alters the offspring ovarian proteome

There were 504 ovarian proteins identified in the D_HP_L offspring who experienced GDM in utero but did not receive the high-fat diet in adulthood. Relative to the D_LP_L offspring ovaries, 85 proteins were reduced and 4 were increased in abundance in the ovaries

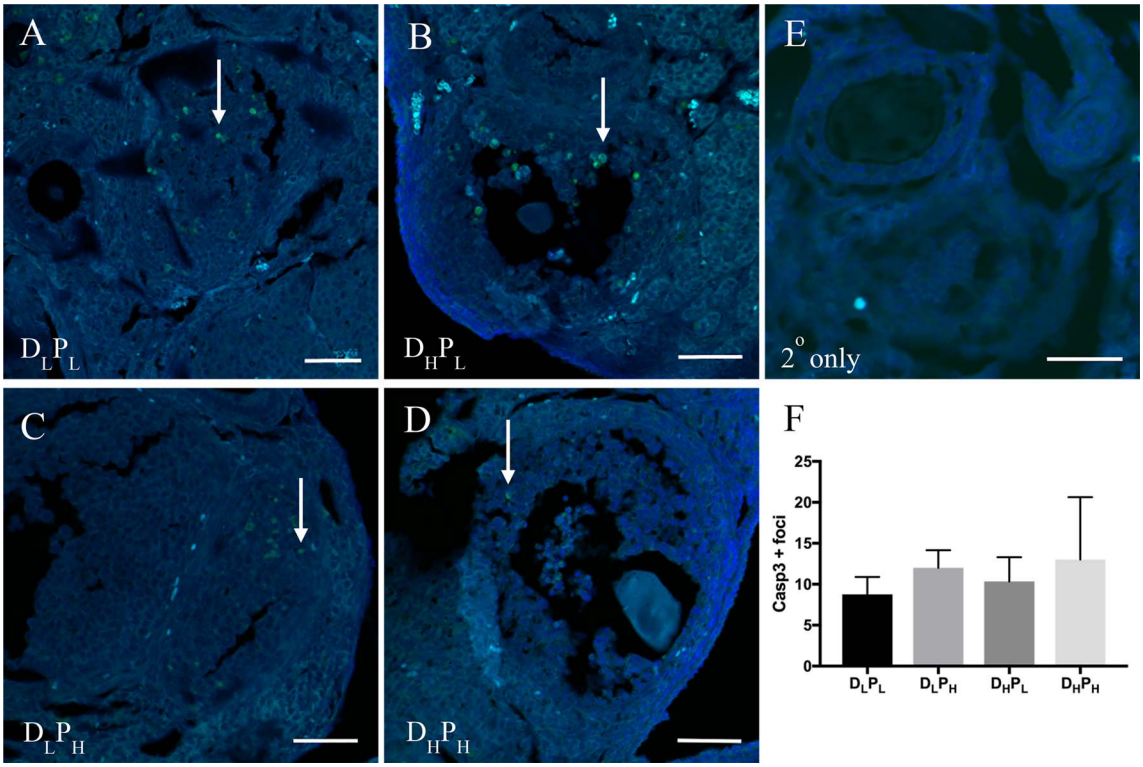

Figure 3. Effect of GDM and/or dietary stress on ovarian cleaved CASP3. A primary antibody directed against cleaved CASP3 was used to determine ovarian localization in (A) D_LP_L; (B) D_HP_L; (C) D_LP_H; and (D) D_HP_H mice. (E) Secondary antibody only control. Green staining indicates cleaved CASP3 while cellular DNA is stained in blue; scale bar = 50 µm. Arrows indicate cleaved CASP3-positive staining in the granulosa cells of secondary follicles. (F) The bars represent mean number of positive CASP3 foci ± SEM; $n = 4$ ovaries per treatment; three sections per ovary.

of D_HP_L mice (log2foldchange ≥ 1 and P-value ≤ 0.1; Figure 4A; Supplementary Table 2).

A high-fat diet affects the ovarian proteome in adult mice

A total of 470 ovarian proteins were identified in the D_LP_H mice. Relative to the D_LP_L offspring ovaries, 30 proteins were decreased and 3 proteins were increased in the ovaries of D_LP_H (log2foldchange ≥ 1 and P-value ≤ 0.1; Figure 4B; Supplementary Table 3).

Additive effect of dietary stress in later life on the proteome of offspring exposed to lean GDM in utero

In the D_HP_H ovaries, 481 total proteins were identified. When compared to the D_LP_L mice, 4 proteins were increased and 87 proteins were decreased, indicating the combined effects of GDM exposure in utero with an HFD stress in adulthood (log2foldchange ≥ 1 and P-value ≤ 0.1; Figure 4C; Supplementary Table 4). Furthermore, comparison of the ovarian proteome of the D_HP_H with the D_LP_H mice revealed the additive effects of in utero GDM since both of these groups experienced the dietary stressor in adulthood, and five proteins were increased and three proteins were decreased (log2foldchange ≥ 1 and P-value ≤ 0.1; Supplementary Table 5).

Of these differentially expressed proteins, 8, 49, and 52 proteins were identified that were unique to D_LP_H, D_HP_L, and D_HP_H, respectively. In addition, 20 proteins were shared between the groups exposed to GDM in utero, 5 proteins were shared between the groups exposed to the HFD, and 14 proteins were shared between all the treatment groups (Figure 5).

Overrepresented GO analysis of maternal GDM exposure in the absence or presence of dietary stress in adulthood.

Proteins identified as being different from the D_LP_L mice (log2foldchange ≥ 1 and P-value ≤ 0.1) in each treatment group (D_LP_H—$n = 33$; D_HP_L—$n = 89$; and D_HP_H—$n = 91$) were assigned to biological process, molecular function, and cellular component using PANTHER GO analysis (Fisher exact with FDR multiple test correction; $P < 0.05$). For biological process, several of the GO categories that showed substantial enrichment in the D_HP_H ovaries relative to controls were associated with a catabolic or metabolic process (Supplementary Figure 1A). There was a 43-fold enrichment of proteins in the D_HP_H ovaries involved in the hydrogen peroxide catabolic process, including the proteins catalase (CAT), apolipoprotein A-IV (APOA4), and peroxiredoxin-5, mitochondrial (PRDX5). Proteins from D_HP_L were enriched in categories related to protein complex disassembly, depolymerization, and regulation of actin filament activity (Supplementary Figure 1B). Actin cross-link formation had the highest fold enrichment in the GDM-only offspring, with proteins such as filamin-A (FLNA) and myristoylated alanine-rich C-kinase substrate (MARCKS) included in the cluster. There were no significant categories assigned in the HFHS diet–alone offspring.

Concerning molecular function, proteins from GDM-exposed and HFHS-fed offspring (D_HP_H) ovaries, and GO categories that were enriched mainly involved enzymatic activity or binding (Supplementary Figure 2A). Transaminase activity included protein-glutamine gamma glutamyltransferase 2 (TGM2) and aspartate

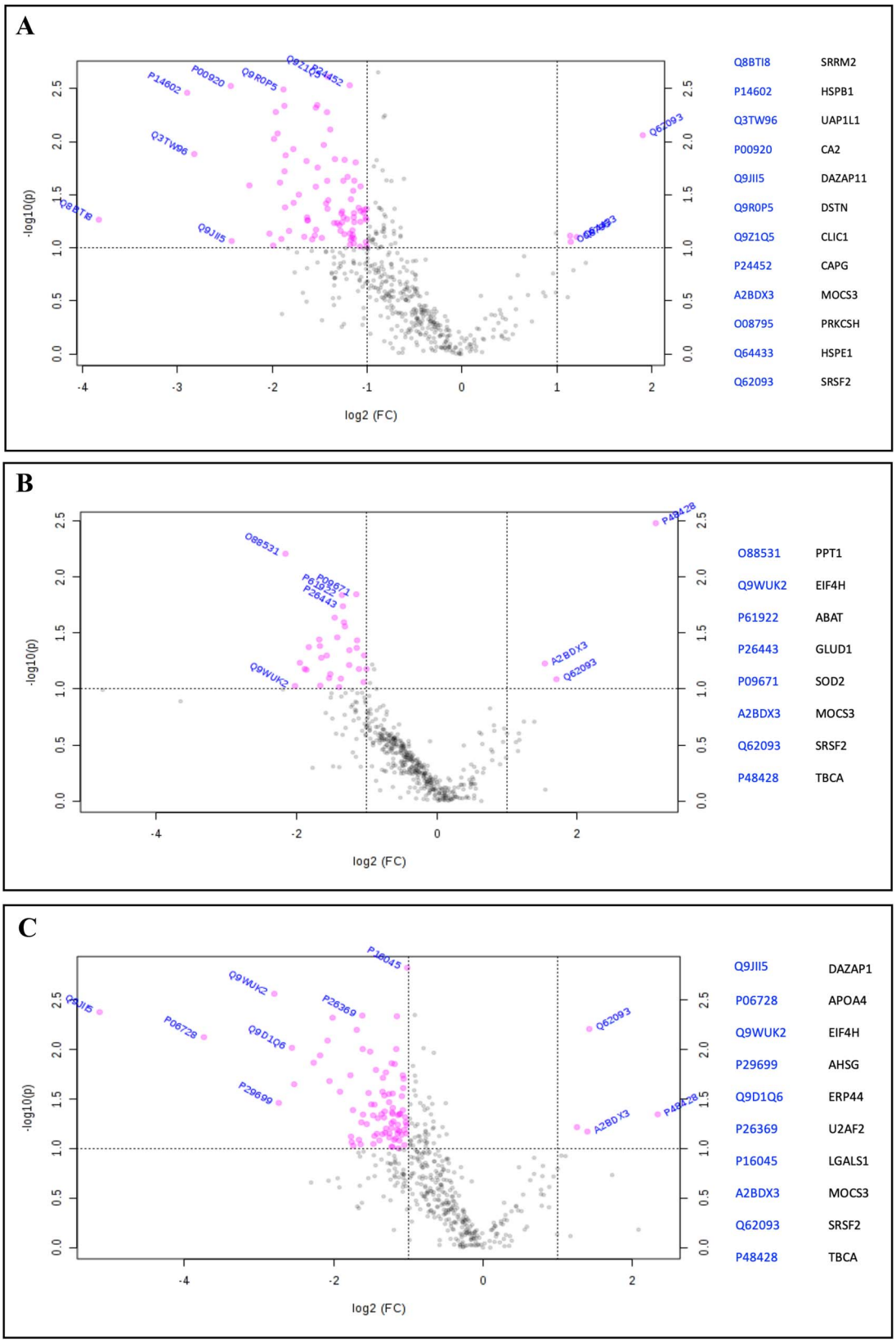

Figure 4. Volcano plots indicating the proteins detected by LC–MS/MS analysis and differing from the $D_L P_L$ group. (A) $D_L P_H$; (B) $D_H P_L$; and (C) $D_H P_H$. The dotted horizontal line shows where $P = 0.1$, with points above the line having $P < 0.1$ and points below having $P > 0.1$. The dotted vertical lines indicate a log2foldchange of $<\pm 1.0$. Pink dots indicate proteins identified that are increased or decreased relative to $D_L P_L$ ovaries; gray dots indicate proteins that did not meet selected thresholds.

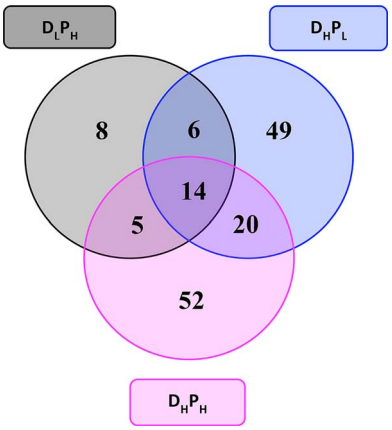

Figure 5. Proteins that are in common or unique between treatments. The Venn diagram presents the number of ovarian proteins identified as being unique to treatment or altered in common by treatment, relative to the D_LP_L group. The number in gray circle indicates the number of proteins identified in the D_LP_H group as being different from the D_LP_L group; the blue circle indicates the number of proteins identified in the D_HP_L group as being different from the D_LP_L group; and the pink circle indicates the number of proteins in the D_HP_H group that differ from the D_LP_L group. Overlapping areas of the circles illustrate the number of proteins that were altered relative to the D_LP_L group by two or more groups.

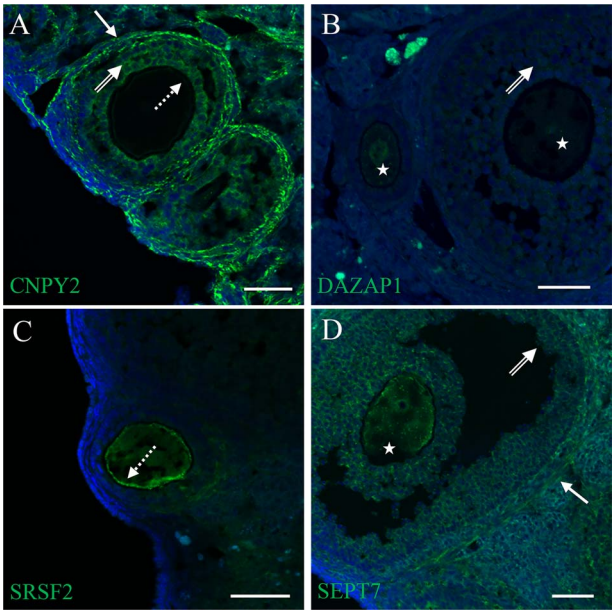

Figure 6. Localization of ovarian proteins by immunofluorescence staining. (A) CNPY2 (20×–1× zoom); (B) DAZAP1(20×–1× zoom); (C) SRSF2 (20×–1× zoom); and (D) SEPT7 (20×–0.5× zoom) proteins were localized in the adult mouse ovary. Green staining indicates the protein of interest, while cellular DNA is stained in blue. Solid arrow indicates theca cells; double-tailed arrow indicates granulosa cells; dotted tail arrow indicates the pericytoplasm region of the oocyte; star indicates oocyte; scale bar = 50 μm.

aminotransferase, mitochondrial (GOT2). Ovaries from females exposed to GDM in utero without a HFHS challenge (D_HP_L) had more binding categories assigned, with the protein kinase C binding category having a 20-fold enrichment (Supplementary Figure 2B). Proteins identified in this category included SRSF2, FLNA, and MARCKS. Similar to the GDM-only group (D_HP_L), the HFHS-only group (D_LP_H) had all identified GO terms associated with binding (Supplementary Figure 2C). Pre-mRNA binding was enriched 61-fold in this group, with SRSF2, polypyrimidine tract-binding protein (PTBP1), and the splicing factor U2AF 65 kda subunit (U2AF2) protein identified in this cluster.

GO terms assigned to cellular component included those involved in cell junctions and various cell complexes. Fascia adherens were enriched 56-fold in the D_HP_H ovaries, with proteins such as vinculin (VCL), alpha-actinin-1 (ACTN1), and spectrin alpha chain, nonerythrocytic 1 (SPTAN1) identified (Supplementary Figure 3A). The interchromatin granule cluster was enriched greater than 100-fold, including the proteins SRSF2 and cleavage and polyadenylation specificity factor subunit 6 (CPSF6) (Supplementary Figure 3B). There were substantially less categories identified in the D_LP_H group. The cytoplasm cluster had the highest enrichment only being enriched by 1.75-fold, containing proteins such as SRSF2, PTBP1, and tubulin-specific chaperone A (TBCA).

Ovarian localization of CNPY2, DAZAP1, SRSF2, and SEPT7

In order to establish the ovarian localization of selected proteins identified to be of interest from the LC–MS/MS analysis, but for whom the ovarian location is unknown, immunofluorescence staining was performed on ovarian sections from adult C57B16/J mice. From the LC–MS/MS analysis, CNPY2 had a log2foldchange of −1.65, −1.72, and −2.18 in groups D_LP_H, D_HP_L, and D_HP_H, respectively. Positive immunofluorescence staining for the CNPY2 protein was observed in the theca and granulosa cells, and the pericytoplasmic region of the oocyte in primary, secondary, and antral follicle stages (Figure 6A).

DAZAP1 had a −2.43 log2foldchange and −5.13 log2foldchange in the D_HP_L and D_HP_H groups, respectively, in the LC–MS/MS analysis but was not altered in the D_LP_H ovaries, suggesting an impact of GDM exposure in utero, and further amplification by dietary stress on ovarian DAZAP1 abundance. Immunological staining for DAZAP1 demonstrated positive staining in the oocyte nucleus, granulosa cells and luteal cells (Figure 6B).

In contrast to the previous proteins selected from our data set, SRSF2 was identified by LC–MS/MS analysis as being increased in groups D_LP_H, D_HP_L, and D_HP_H with log2foldchange of 1.70, 1.91, and 1.42, respectively, relative to the D_LP_L ovaries. SRSF2 protein was determined by immunofluorescence staining to be localized to the oocyte pericytoplasmic region and nucleus in preovulatory follicles (Figure 6C).

SEPT7 was noted from the LC–MS/MS analysis to be decreased in the D_LP_H, D_HP_L, and D_HP_H ovaries by −1.04, −1.43, and −1.07 log2foldchange, respectively. Positive immunofluorescence staining for SEPT7 was observed in the oocyte, granulosa, and theca cells of primary, secondary, and antral follicles (Figure 6D).

Discussion

The reproductive phenotypic impacts of obesity and insulin resistance have been well characterized, yet the percentage of the population at risk continues to increase [45]. In parallel with rising obesity rates, the number of women acquiring GDM is also increasing [46]. One of the major risk factors for GDM development is pregestational obesity and/or insulin resistance, although interestingly around a third of cases occur in lean women [47].

While the underlying etiology of GDM remains unknown, several experimental animal models have been developed that effectively mimic the most common GDM features. Partial pancreatectomy in postpubertal rodents results in a mild type 1 diabetes phenotype via the reduction of β-cell numbers, but limitations include the latency for diabetic symptoms to appear [48]. Administration of alloxan and streptozotocin (STZ) impairs and destroys pancreatic β cells, leading to hyperglycemia and insulin insufficiency [49–51]. Nicotinamide (NA) injection prior to STZ administration protects the pancreas from severe damage and leads to a lower number of fetal malformations [52–54]. Mouse models of GDM are also available via gene knockout or transgenic overexpression, but although effective at emulating GDM, many of these genetic models have more severe phenotypes than typically observed in human cases of GDM, and the genetic changes may be passed on to offspring. A commonly used GDM mouse model are females who are heterozygous for a mutation in the leptin receptor (ObR; $Db^{\pm}$), who have reduced glucose homeostasis in the nonpregnant state, but spontaneously develop hyperphagic feeding, increased adiposity, insulin resistance, and glucose intolerance during pregnancy [55], although conflicting results have been noted in other studies [56–58].

Another approach for inducing GDM is via dietary manipulation. Dams consuming a high-fat diet to induce obesity and insulin resistance prepregnancy have a GDM phenotype during pregnancy [59–63]. The maternal model utilized in our study is also diet induced and includes a high-fat and high-sugar diet, which is comparable to the diet of the human population, but obesity is absent prior to gestation. With this method, we are able to elucidate the mechanisms behind GDM without the additive effects of obesity. These females exhibit susceptibility to glucose intolerance later in life when challenged with the same diet but in the absence of increased body mass [41]. An obvious drawback with using this model is that there is a confounding effect of differing dietary composition, and the HFHS mice in this study received an additional fat source to the controls in the form of sunflower oil. Future studies aimed at assessing any additive impacts of differing fat source on the ovarian endpoints measured are possible in the future, though it is far more plausible that it is the increased adiposity in this model that contributes to the ovarian effects reported herein.

The ramifications of GDM and the health of the offspring also need consideration. In addition to risk of stillbirth, babies born to mothers who experience diabetes during pregnancy have higher rates of macrosomia [35], hypoglycemia [36], respiratory distress [36], future obesity [37], and like the mother, a predisposition for type 2 diabetes later in life [38]. Offspring that were exposed to our model of GDM in utero and later on challenged with the HFHS diet had increased body weight, higher body fat percentage, and increased adipose insulin sensitivity [42]. Reproductive effects on the male offspring from these dams included reduced sperm counts, reduced germ cell apoptosis, and low testosterone [64]. Our results in the female offspring corroborate the reproductive effects noted in the males, with reduced numbers of healthy primary and secondary follicle numbers, as well as a numerical decrease in primordial follicle numbers in the D_HP_H mice illustrating that in utero environment coupled with a later stressor in adulthood may have negative impacts on female fertility.

Previous work from our group and others has demonstrated how the metabolic changes that occur during obesity can alter folliculogenesis and the responsive pathways [15, 16, 19, 65–67]. The ovarian PI3K-PTEN-AKT-FOXO3 signaling pathway is involved in follicular activation via an insulin-mediated process [68, 69]. Hyperinsulinemia is common during obesity, and from this, we have previously reported changes in the activation of the PI3K pathway, resulting in increased follicular activation [14]. Thus, it is possible that the observed lower number of follicles in the GDM offspring, especially those challenged with the high-fat diet later in life, result from the increased body mass and insulin resistance following in utero metabolic exposures. In this study, the female mice had increased adiposity as measured by nuclear magnetic resonance imaging as early as 4 weeks of age, despite not being introduced to the HFHS diet until 23 weeks of age [42]. A subject for future analysis would be to define at what rate the introduction of the HFHS diet to GDM offspring diminishes the follicular pool subsequent to GDM exposure alone.

Obesity is also associated with ovarian DNA damage [17, 18, 40] and throughout the body [70]. Interestingly, we did not observe any consequential changes on GDM and/or dietary stress in later life in the abundance of γH2AX, which is considered the gold standard for DNA double strand break localization [71]. As with increased DNA damage detected in obesity, increased granulosa cell apoptosis has also been reported [72]. We did not, however, observe increased granulosa cell apoptosis as detected by cleaved CASP3 protein in our offspring ovaries. The lack of additional DNA damage and cellular apoptosis in our model could be interpreted as that while they have increased body weight and insulin sensitivity, they have not necessarily amassed a metabolic syndrome severe enough to trigger a genotoxic response. This remains to be determined.

Proteomic profiling can be highly informative in investigating alterations to proteins due to a defined environmental and pathological treatment. In an unbiased proteomic approach, we identified several proteins of interest, including DAZAP1, SEPT7, CNPY2, and SRSF2, to be altered by GDM, adult dietary stress, or both. DAZAP1 was substantially decreased in ovaries from female mice exposed to GDM in utero and further impacted by the additional insult of the HFHS diet. The deleted in azoospermia (DAZ) family of proteins are present in male and female germ cells and play a major role in germ cell development and fertility [73]. Mutations in DAZAP1 result in perinatal lethality, with those surviving experiencing reproductive defects such as sterility as well as growth retardation [74]. Fertility defects associated with DAZAP1 have been typically described in males [75, 76], so our finding of alterations to DAZAP1 due to in utero GDM and dietary stress and localization in granulosa and luteal cells as well as in the oocyte implies that DAZAP1 may have important roles in ovarian physiology and female fertility through altering follicle growth and survival, potentially contributing to POI.

The septin family of proteins have been well characterized as being involved in the spindle positioning and cell division [77–79]. Loss of SEPT7 results in improper spindle organization in the oocyte and disruption of chromosome alignment affecting progression of meiosis [61]. Poor oocyte quality is attributed with increased body mass [10], and the modest decrease in SEPT7 observed in our study suggests that the metabolic stress from a HFHS diet, GDM exposure in utero, or both may affect oocyte quality and/or maturation. SEPT7 was also identified in our enriched cellular component GO analysis in both the GDM-exposed groups as septin complex, septin ring, and septin cytoskeleton. In agreement with this possibility, localization of SEPT7 within the follicle and the oocyte further implicates SEPT7 as an essential player in murine oocyte meiotic maturation, and that SEPT7 is vulnerable to alteration due to metabolic alterations.

CNPY2 is pivotal in the induction of the PERK–CHOP unfolded protein response (UPR) response pathway, which is a highly conserved quality control mechanism for cells that are under

endoplasmic reticulum (ER) stress [80]. The luminal chaperone GRP78 dissociates from PERK and CNPY2 during ER stress and unfolded protein accumulation, facilitating the initiation of the UPR response [80]. Furthermore, *Cnpy2* is differentially expressed in human placental tissue from GDM pregnancies, though these results revealed a positive fold change [81] in contrast with our findings of decreased CNPY2 protein abundance. We also determined the localization of CNPY2, with positive immunoreactivity in the theca cells, granulosa cells, and in the pericytoplasm of the oocyte.

Also associated with the cellular stress response is SRSF2, which is increased during genotoxic stress [82] and is increased across all treatment groups in our study and was also assigned to several of the GO categories that were highly enriched. SRSF2 is an alternative splicing factor involved in the regulation of apoptotic caspases, with the mechanism for proapoptotic or antiapoptotic caspases determined by the numerous splice variants [83]. Immunohistochemical analysis of SRSF2 revealed expression in the pericytoplasm of the oocyte, though analysis of cleaved CASP3 revealed no differences in the levels of apoptotic cells between any of the groups, so increased SRSF2 observed in this study may not be substantial enough to generate a proapoptotic response via CASP3. Conversely, SRSF2 may be functioning in an antiapoptotic response to the metabolic conditions arising from increasing adiposity and/or insulin resistance.

In conclusion, these study findings indicate the impact of GDM and HFHS diets on follicle number and the ovarian proteome and illustrate that GDM sensitizes the offspring ovary to a dietary HFHS stress later in life, consequentially impacting the number of healthy follicles. Further, the altered abundance of ovarian proteins in offspring exposed to maternal GDM emphasizes the potential long-term effects of metabolic alterations in utero on ovarian function in the absence of obesity. Many of the proteins identified are those for which we have little understanding of their ovarian function and lay the foundation for future studies to determine their ovarian importance. Taken together, these findings illustrate a possible impact on fertility and oocyte quality provided in a two-hit stress model relative to GDM exposure in utero and in response to a western diet later in life and support a developmental origin of ovarian disorder (DOOD).

Supplementary data

Supplementary data are available at *BIOLRE* online.

Conflict of Interest

The authors have declared that no conflict of interest exists.

References

1. Hirshfield AN. Development of follicles in the mammalian ovary. *Int Rev Cytol* 1991; **124**:43–101.
2. Coulam CB, Adamson SC, Annegers JF. Incidence of premature ovarian failure. *Obstet Gynecol* 1986; **67**:604–606.
3. Sullivan SD, Sarrel PM, Nelson LM. Hormone replacement therapy in young women with primary ovarian insufficiency and early menopause. *Fertil Steril* 2016; **106**:1588–1599.
4. Colditz GA, Willett WC, Rotnitzky A, Manson JE. Weight gain as a risk factor for clinical diabetes mellitus in women. *Ann Intern Med* 1995; **122**:481–486.
5. Lavie CJ, Milani RV, Ventura HO. Obesity and cardiovascular disease: risk factor, paradox, and impact of weight loss. *J Am Coll Cardiol* 2009; **53**:1925–1932.
6. Cozzo AJ, Fuller AM, Makowski L. Contribution of adipose tissue to development of cancer. *Compr Physiol* 2017; **8**:237–282.
7. Gesink Law DC, Maclehose RF, Longnecker MP. Obesity and time to pregnancy. *Hum Reprod* 2007; **22**:414–420.
8. Shrestha A, Olsen J, Ramlau-Hansen CH, Bech BH, Nohr EA. Obesity and age at menarche. *Fertil Steril* 2011; **95**:2732–2734.
9. Dravecka I, Lazurova I, Kraus V. Obesity is the major factor determining an insulin sensitivity and androgen production in women with anovulary cycles. *Bratisl Lek Listy* 2003; **104**:393–399.
10. Metwally M, Cutting R, Tipton A, Skull J, Ledger WL, Li TC. Effect of increased body mass index on oocyte and embryo quality in IVF patients. *Reprod Biomed Online* 2007; **15**:532–538.
11. Brewer CJ, Balen AH. The adverse effects of obesity on conception and implantation. *Reproduction* 2010; **140**:347–364.
12. Chu SY, Callaghan WM, Kim SY, Schmid CH, Lau J, England LJ, Dietz PM. Maternal obesity and risk of gestational diabetes mellitus. *Diabetes Care* 2007; **30**:2070–2076.
13. Sheffield JS, Butler-Koster EL, Casey BM, McIntire DD, Leveno KJ. Maternal diabetes mellitus and infant malformations. *Obstet Gynecol* 2002; **100**:925–930.
14. Nteeba J, Ross JW, Perfield JW 2nd, Keating AF. High fat diet induced obesity alters ovarian phosphatidylinositol-3 kinase signaling gene expression. *Reprod Toxicol* 2013; **42**:68–77.
15. Nteeba J, Ganesan S, Keating AF. Progressive obesity alters ovarian folliculogenesis with impacts on pro-inflammatory and steroidogenic signaling in female mice. *Biol Reprod* 2014; **91**:86.
16. Nteeba J, Ganesan S, Madden JA, Dickson MJ, Keating AF. Progressive obesity alters ovarian insulin, phosphatidylinositol-3 kinase, and chemical metabolism signaling pathways and potentiates ovotoxicity induced by phosphoramide mustard in mice. *Biol Reprod* 2017; **96**:478–490.
17. Ganesan S, Nteeba J, Keating AF. Enhanced susceptibility of ovaries from obese mice to 7,12-dimethylbenz [a]anthracene-induced DNA damage. *Toxicol Appl Pharmacol* 2014; **281**:203–210.
18. Ganesan S, Nteeba J, Madden JA, Keating AF. Obesity alters phosphoramide mustard-induced ovarian DNA repair in mice. *Biol Reprod* 2017; **96**:491–501.
19. Nteeba J, Ganesan S, Keating AF. Impact of obesity on ovotoxicity induced by 7,12-dimethylbenz [a] anthracene in mice. *Biol Reprod* 2014; **90**:68.
20. Huang HY, Chen HL, Feng LP. Maternal obesity and the risk of neural tube defects in offspring: a meta-analysis. *Obes Res Clin Pract* 2017; **11**:188–197.
21. Hanafi MY, Saleh MM, Saad MI, Abdelkhalek TM, Kamel MA. Transgenerational effects of obesity and malnourishment on diabetes risk in F2 generation. *Mol Cell Biochem* 2016; **412**:269–280.
22. Grissom NM, Lyde R, Christ L, Sasson IE, Carlin J, Vitins AP, Simmons RA, Reyes TM. Obesity at conception programs the opioid system in the offspring brain. *Neuropsychopharmacology* 2014; **39**:801–810.
23. Radulescu L, Ferechide D, Popa F. The importance of fetal gender in intrauterine growth restriction. *J Med Life* 2013; **6**:38–39.
24. Desai M, Jellyman JK, Han G, Beall M, Lane RH, Ross MG. Maternal obesity and high-fat diet program offspring metabolic syndrome. *Am J Obstet Gynecol* 2014; **211**:237.e1–237.e13.
25. Aiken CE, Tarry-Adkins JL, Ozanne SE. Transgenerational effects of maternal diet on metabolic and reproductive ageing. *Mamm Genome* 2016; **27**:430–439.
26. Aiken CE, Tarry-Adkins JL, Penfold NC, Dearden L, Ozanne SE. Decreased ovarian reserve, dysregulation of mitochondrial biogenesis, and increased lipid peroxidation in female mouse offspring exposed to an obesogenic maternal diet. *Faseb J* 2016; **30**:1548–1556.
27. Chan KA, Tsoulis MW, Sloboda DM. Early-life nutritional effects on the female reproductive system. *J Endocrinol* 2015; **224**:R45–R62.
28. Connor KL, Vickers MH, Beltrand J, Meaney MJ, Sloboda DM. Nature, nurture or nutrition? Impact of maternal nutrition on maternal care, offspring development and reproductive function. *J Physiol* 2012; **590**:2167–2180.
29. Noctor E, Dunne FP. Type 2 diabetes after gestational diabetes: the influence of changing diagnostic criteria. *World J Diabetes* 2015; **6**:234–244.

30. Reece EA, Leguizamon G, Wiznitzer A. Gestational diabetes: the need for a common ground. *Lancet* 2009; **373**:1789–1797.
31. Kuhl C. Insulin secretion and insulin resistance in pregnancy and GDM. Implications for diagnosis and management. *Diabetes* 1991; **40** Suppl 2:18–24.
32. Yogev Y, Xenakis EM, Langer O. The association between preeclampsia and the severity of gestational diabetes: the impact of glycemic control. *Am J Obstet Gynecol* 2004; **191**:1655–1660.
33. Bellamy L, Casas JP, Hingorani AD, Williams D. Type 2 diabetes mellitus after gestational diabetes: a systematic review and meta-analysis. *Lancet* 2009; **373**:1773–1779.
34. Kim C. Maternal outcomes and follow-up after gestational diabetes mellitus. *Diabet Med* 2014; **31**:292–301.
35. Wang C, Zhu W, Wei Y, Feng H, Su R, Yang H. Exercise intervention during pregnancy can be used to manage weight gain and improve pregnancy outcomes in women with gestational diabetes mellitus. *BMC Pregnancy Childbirth* 2015; **15**:255.
36. Gasim T. Gestational diabetes mellitus: maternal and perinatal outcomes in 220 saudi women. *Oman Med J* 2012; **27**:140–144.
37. Nehring I, Chmitorz A, Reulen H, von Kries R, Ensenauer R. Gestational diabetes predicts the risk of childhood overweight and abdominal circumference independent of maternal obesity. *Diabet Med* 2013; **30**:1449–1456.
38. Vohr BR, Boney CM. Gestational diabetes: the forerunner for the development of maternal and childhood obesity and metabolic syndrome? *J Matern Fetal Neonatal Med* 2008; **21**:149–157.
39. Nteeba J, Ortinau LC, Perfield JW 2nd, Keating AF. Diet-induced obesity alters immune cell infiltration and expression of inflammatory cytokine genes in mouse ovarian and peri-ovarian adipose depot tissues. *Mol Reprod Dev* 2013; **80**:948–958.
40. Ganesan S, Nteeba J, Keating AF. Impact of obesity on 7,12-dimethylbenz [a]anthracene-induced altered ovarian connexin gap junction proteins in female mice. *Toxicol Appl Pharmacol* 2015; **282**:1–8.
41. Pennington KA, van der Walt N, Pollock KE, Talton OO, Schulz LC. Effects of acute exposure to a high-fat, high-sucrose diet on gestational glucose tolerance and subsequent maternal health in mice. *Biol Reprod* 2017; **96**:435–445.
42. Talton OO, Bates K, Salazar SR, Ji T, Schulz LC. Lean maternal hyperglycemia alters offspring lipid metabolism and susceptibility to diet-induced obesity in mice. *Biol Reprod* 2019; **100**(**5**):1356–1369.
43. Xia J, Sinelnikov IV, Han B, Wishart DS. MetaboAnalyst 3.0—making metabolomics more meaningful. *Nucleic Acids Res* 2015; **43**:W251–W257.
44. Xia J, Wishart DS. Using MetaboAnalyst 3.0 for comprehensive metabolomics data analysis. *Curr Protoc Bioinformatics* 2016; **55**:14.10.11–14.10.91.
45. Broughton DE, Moley KH. Obesity and female infertility: potential mediators of obesity's impact. *Fertil Steril* 2017; **107**:840–847.
46. Barbour LA. Unresolved controversies in gestational diabetes: implications on maternal and infant health. *Curr Opin Endocrinol Diabetes Obes* 2014; **21**:264–270.
47. Blickstein I, Doyev R, Trojner Bregar A, Brzan Simenc G, Verdenik I, Tul N. The effect of gestational diabetes, pre-gravid maternal obesity, and their combination ('diabesity') on outcomes of singleton gestations. *J Matern Fetal Neonatal Med* 2018; **31**:640–643.
48. Foglia VG, Cattaneo de Peralta R, Ibarra R, Rivera Cortes L. Fetal and placental characteristics of pregnancy in pancreatectomized rats. *Rev Soc Argent Biol* 1967; **43**:187–198.
49. Junod A, Lambert AE, Stauffacher W, Renold AE. Diabetogenic action of streptozotocin: relationship of dose to metabolic response. *J Clin Invest* 1969; **48**:2129–2139.
50. Tsai MY, Schallinger LE, Josephson MW, Brown DM. Disturbance of pulmonary prostaglandin metabolism in fetuses of alloxan-diabetic rabbits. *Biochim Biophys Acta* 1982; **712**:395–399.
51. Kiss AC, Lima PH, Sinzato YK, Takaku M, Takeno MA, Rudge MV, Damasceno DC. Animal models for clinical and gestational diabetes: maternal and fetal outcomes. *Diabetol Metab Syndr* 2009; **1**:21.
52. Masiello P, Broca C, Gross R, Roye M, Manteghetti M, Hillaire-Buys D, Novelli M, Ribes G. Experimental NIDDM: development of a new model in adult rats administered streptozotocin and nicotinamide. *Diabetes* 1998; **47**:224–229.
53. John CM, Ramasamy R, Al Naqeeb G, Al-Nuaimi AH, Adam A. Nicotinamide supplementation protects gestational diabetic rats by reducing oxidative stress and enhancing immune responses. *Curr Med Chem* 2012; **19**:5181–5186.
54. Abdul Aziz SH, John CM, Mohamed Yusof NI, Nordin M, Ramasamy R, Adam A, Mohd Fauzi F. Animal model of gestational diabetes mellitus with pathophysiological resemblance to the human condition induced by multiple factors (nutritional, pharmacological, and stress) in rats. *Biomed Res Int* 2016; **2016**:9704607.
55. Kaufmann RC, Amankwah KS, Dunaway G, Maroun L, Arbuthnot J, Roddick JW, Jr. An animal model of gestational diabetes. *Am J Obstet Gynecol* 1981; **141**:479–482.
56. Harrod JS, Rada CC, Pierce SL, England SK, Lamping KG. Altered contribution of RhoA/Rho kinase signaling in contractile activity of myometrium in leptin receptor-deficient mice. *Am J Physiol Endocrinol Metab* 2011; **301**:E362–E369.
57. Pollock KE, Stevens D, Pennington KA, Thaisrivongs R, Kaiser J, Ellersieck MR, Miller DK, Schulz LC. Hyperleptinemia during pregnancy decreases adult weight of offspring and is associated with increased offspring Locomotor activity in mice. *Endocrinology* 2015; **156**:3777–3790.
58. Plows JF, Yu X, Broadhurst R, Vickers MH, Tong C, Zhang H, Qi H, Stanley JL, Baker PN. Absence of a gestational diabetes phenotype in the LepRdb/+ mouse is independent of control strain, diet, misty allele, or parity. *Sci Rep* 2017; **7**:.
59. Holemans K, Caluwaerts S, Poston L, Van Assche FA. Diet-induced obesity in the rat: a model for gestational diabetes mellitus. *Am J Obstet Gynecol* 2004; **190**:858–865.
60. Liang C, DeCourcy K, Prater MR. High-saturated-fat diet induces gestational diabetes and placental vasculopathy in C57BL/6 mice. *Metabolism* 2010; **59**:943–950.
61. Li S, Ou XH, Wei L, Wang ZB, Zhang QH, Ouyang YC, Hou Y, Schatten H, Sun QY. Septin 7 is required for orderly meiosis in mouse oocytes. *Cell Cycle* 2012; **11**:3211–3218.
62. Ford SP, Zhang L, Zhu M, Miller MM, Smith DT, Hess BW, Moss GE, Nathanielsz PW, Nijland MJ. Maternal obesity accelerates fetal pancreatic beta-cell but not alpha-cell development in sheep: prenatal consequences. *Am J Physiol Regul Integr Comp Physiol* 2009; **297**:R835–R843.
63. Moore MC, Menon R, Coate KC, Gannon M, Smith MS, Farmer B, Williams PE. Diet-induced impaired glucose tolerance and gestational diabetes in the dog. *J Appl Physiol (1985)* 2011; **110**:458–467.
64. Mao J, Pennington KA, Talton OO, Schulz LC, Sutovsky M, Lin Y, Sutovsky P. In utero and postnatal exposure to high fat, high sucrose diet suppressed testis apoptosis and reduced sperm count. *Sci Rep* 2018; **8**:7622.
65. Wang N, Luo LL, Xu JJ, Xu MY, Zhang XM, Zhou XL, Liu WJ, Fu YC. Obesity accelerates ovarian follicle development and follicle loss in rats. *Metabolism* 2014; **63**:94–103.
66. Akamine EH, Marcal AC, Camporez JP, Hoshida MS, Caperuto LC, Bevilacqua E, Carvalho CR. Obesity induced by high-fat diet promotes insulin resistance in the ovary. *J Endocrinol* 2010; **206**:65–74.
67. Wu S, Divall S, Wondisford F, Wolfe A. Reproductive tissues maintain insulin sensitivity in diet-induced obesity. *Diabetes* 2012; **61**:114–123.
68. John GB, Gallardo TD, Shirley LJ, Castrillon DH. Foxo3 is a PI3K-dependent molecular switch controlling the initiation of oocyte growth. *Dev Biol* 2008; **321**:197–204.
69. Reddy P, Liu L, Adhikari D, Jagarlamudi K, Rajareddy S, Shen Y, Du C, Tang W, Hamalainen T, Peng SL, Lan ZJ, Cooney AJ et al. Oocyte-specific deletion of Pten causes premature activation of the primordial follicle pool. *Science* 2008; **319**:611–613.
70. Zaki M, Basha W, El-Bassyouni HT, El-Toukhy S, Hussein T. Evaluation of DNA damage profile in obese women and its association to risk of metabolic syndrome, polycystic ovary syndrome and recurrent preeclampsia. *Genes Dis* 2018; **5**:367–373.

71. Fernandez-Capetillo O, Lee A, Nussenzweig M, Nussenzweig A. H2AX: the histone guardian of the genome. *DNA Repair (Amst)* 2004; **3**:959–967.
72. Walzem RL, Chen SE. Obesity-induced dysfunctions in female reproduction: lessons from birds and mammals. *Adv Nutr* 2014; **5**:199–206.
73. Fu XF, Cheng SF, Wang LQ, Yin S, De Felici M, Shen W. DAZ family proteins, key players for germ cell development. *Int J Biol Sci* 2015; **11**:1226–1235.
74. Hsu LC, Chen HY, Lin YW, Chu WC, Lin MJ, Yan YT, Yen PH. DAZAP1, an hnRNP protein, is required for normal growth and spermatogenesis in mice. *RNA* 2008; **14**:1814–1822.
75. Dai T, Vera Y, Salido EC, Yen PH. Characterization of the mouse Dazap1 gene encoding an RNA-binding protein that interacts with infertility factors DAZ and DAZL. *BMC Genomics* 2001; **2**:6.
76. Tsui S, Dai T, Roettger S, Schempp W, Salido EC, Yen PH. Identification of two novel proteins that interact with germ-cell-specific RNA-binding proteins DAZ and DAZL1. *Genomics* 2000; **65**:266–273.
77. Spiliotis ET, Kinoshita M, Nelson WJ. A mitotic septin scaffold required for mammalian chromosome congression and segregation. *Science* 2005; **307**:1781–1785.
78. Kadota J, Yamamoto T, Yoshiuchi S, Bi E, Tanaka K. Septin ring assembly requires concerted action of polarisome components, a PAK kinase Cla4p, and the actin cytoskeleton in *Saccharomyces cerevisiae*. *Mol Biol Cell* 2004; **15**:5329–5345.
79. Enserink JM, Smolka MB, Zhou H, Kolodner RD. Checkpoint proteins control morphogenetic events during DNA replication stress in *Saccharomyces cerevisiae*. *J Cell Biol* 2006; **175**:729–741.
80. Hong F, Liu B, Wu BX, Morreall J, Roth B, Davies C, Sun S, Diehl JA, Li Z. CNPY2 is a key initiator of the PERK-CHOP pathway of the unfolded protein response. *Nat Struct Mol Biol* 2017; **24**:834–839.
81. Enquobahrie DA, Williams MA, Qiu C, Meller M, Sorensen TK. Global placental gene expression in gestational diabetes mellitus. *Am J Obstet Gynecol* 2009; **200**:206.e201–206.e213.
82. Merdzhanova G, Edmond V, De Seranno S, Van den Broeck A, Corcos L, Brambilla C, Brambilla E, Gazzeri S, Eymin B. E2F1 controls alternative splicing pattern of genes involved in apoptosis through upregulation of the splicing factor SC35. *Cell Death Differ* 2008; **15**:1815–1823.
83. Kedzierska H, Piekielko-Witkowska A. Splicing factors of SR and hnRNP families as regulators of apoptosis in cancer. *Cancer Lett* 2017; **396**:53–65.